Can. J. Remote Sensing, Vol. 34, Suppl. 2, pp. S385–S397, 2008

Modeling the hemispherical scanning, below-canopy lidar and vegetation structure characteristics with a geometric-optical and radiative-transfer model

Wenge Ni-Meister, Alan H. Strahler, Curtis E. Woodcock, Crystal B. Schaaf, David L.B. Jupp, Tian Yao, Feng Zhao, and Xiaoyuan Yang

Abstract. This study applied a hybrid canopy geometric optical and radiative transfer (GORT) model to study the vegetation structure characteristics and lidar signals from a terrestrial below-canopy lidar instrument, Echidna Validation Instrument (EVI), developed by CSIRO Australia. Off-nadir scans from the below-canopy lidar show strong laser energy returns from both leaves and tree trunks. The GORT model was modified to include the effect of both leaves and trunks on below-canopy lidar energy returns by treating the trunks as simple uniform cylinders extending to the middle of each tree crown. GORT was also extended to allow multiple canopy layers by convolution of the canopy gap probability profiles for individual canopy layers. The extended leaf-and-trunk GORT model was evaluated by comparing the modeled and EVI-derived gap probability profiles in a single-layer pine plantation and a two-layer eucalypt forest at the Tumbarumba flux tower site in southeastern New South Wales, Australia. Results show that the new leaf-and-trunk GORT model improves estimates of EVI-derived gap probability profiles. This study demonstrates the potential use of terrestrial upward-scanning hemispherical lidar to retrieve forest canopy structural information. A future goal is to link these terrestrial hemispherical lidar measurements to downward-looking airborne lidar, such as the Laser Vegetation Imaging Sensor (LVIS), and spaceborne lidar, such as the Geoscience Laser Altimeter System (GLAS) on ICESat, through a common model to provide large-area mapping of vegetation structural properties and biomass.

Résumé. Dans cette étude, nous appliquons un modèle géométrique-optique hybride de transfert radiatif du couvert (GORT) pour étudier les caractéristiques de la structure de la végétation et les signaux lidar acquis par un instrument lidar terrestre opérant sous le couvert, l'EVI (« Echidna Validation Instrument »), développé par CSIRO Australia. Des balayages en visée oblique réalisés avec le lidar opérant sous le couvert montrent des retours d'énergie lidar forts à partir des feuilles et des troncs d'arbres. Le modèle GORT a été modifié pour inclure l'effet des feuilles et des troncs sur les retours d'énergie lidar sous le couvert en traitant les troncs comme de simples cylindres uniformes s'étendant jusqu'au milieu de la couronne de chaque arbre. Le modèle GORT a aussi été élargi pour permettre des couches de couvert multiples par convolution des profils de probabilité des trouées dans le couvert pour les couches de couvert individuelles. Le modèle élargi GORT des feuilles et des troncs a été évalué en comparant les profils de probabilité des trouées modélisés et ceux dérivés d'EVI dans une plantation de pins à couche unique et une forêt d'eucalyptus à deux couches sur le site de la tour de flux de Tumbarumba, dans le sud-ouest de New South Wales, en Australie. Les résultats montrent que le nouveau modèle GORT des feuilles et des troncs améliore les estimations des profils de probabilité des trouées dérivés par EVI. Cette étude démontre le potentiel de l'utilisation du lidar hémisphérique à balayage vers le haut pour l'extraction de l'information structurelle du couvert de la forêt. Un des objectifs futurs est de relier ces mesures terrestres lidar hémisphériques aux mesures lidar aéroportées à visée vers le bas, comme le LVIS (« Laser Vegetation Imaging Sensor »), et le lidar satellitaire, comme le GLAS (« Geoscience Laser Altimeter System ») sur ICESat, par le biais d'un modèle commun pour obtenir une cartographie à grande échelle des propriétés structurelles de la végétation et de la biomasse.
[Traduit par la Rédaction]

Received 22 February 2008. Accepted 28 June 2008. Published on the *Canadian Journal of Remote Sensing* Web site at http://pubs.nrc-cnrc.gc.ca/cjrs on 28 November 2008.

W. Ni-Meister.[1] Department of Geography, Hunter College of The City University of New York, New York, NY 10065, USA.

A.H. Strahler, C.E. Woodcock, C.B. Schaaf, T. Yao, F. Zhao, and X. Yang. Department of Geography and Environment, Boston University, Boston, MA 21005, USA.

D.L.B. Jupp. CSIRO Marine and Atmospheric Research, Canberra ACT 2601, Australia.

[1]Corresponding author (e-mail: Wenge.Ni-Meister@hunter.cuny.edu).

Introduction

Remote estimation of vegetation structure characteristics and forest biomass has become essential to ecosystem modeling studies and the advance in understanding of many ecosystem processes. An advantage over many remote sensing measurements, vegetation lidars provide direct and indirect measurements of vegetation structure (Dubayah and Drake, 2000). Recent advances in lidar technology have made a great deal of vegetation lidar data available to study the link between vegetation lidar signals and vegetation structure characteristics. The spaceborne Geoscience Laser Altimeter System (GLAS), part of the ICESat mission, provides global lidar data with a 70 m footprint (Zwally et al., 2002). Airborne data, collected using a Scanning Lidar Imager of Canopies by Echo Recovery (SLICER) with a 15 m footprint and Laser Vegetation Imaging Sensor (LVIS) with a 25 m footprint, have also been acquired over several large areas for improved vegetation structure characterization (Blair et al., 1999). Small-footprint lidar data have also been collected in many small regions of the globe (Jupp et al., 2005). These global, regional, and local lidar data can provide the detailed vegetation structure data necessary for carbon models and ecosystem processes studies.

Many studies have demonstrated the potential use of spaceborne and airborne downward-scanning above-canopy vegetation lidar data to map vegetation height, above-ground biomass characteristics, and other vegetation structure parameters (Lefsky et al., 1999; 2002; 2005; Harding et al., 2001; Harding and Carabajal, 2005; Drake et al., 2002a; 2002b; 2003; Nelson et al., 1984; 2003; Patenaude et al., 2004; Means et al., 1999). However, the ability of nadir viewing downward-scanning above-canopy lidar to retrieve vegetation structure is somewhat limited due to the narrow extent of its swath. Many woody structure characteristics are therefore not directly measured, except for vegetation height. All other vegetation structure parameters must be indirectly derived. For example, above-ground biomass has been indirectly derived from empirical relationships with lidar-measured vegetation height (Lefsky et al., 2005) or accumulated vegetation lidar returns (Drake et al., 2002a; 2002b; 2003). Often, these relationships are site dependent and lead to large uncertainties when applied to large regions. Another limitation of even full waveform downward-scanning above-canopy lidar is that it provides only an effective foliage profile, not the direct measure of foliage biomass (Ni-Meister et al., 2001), and the ratio of the ground and canopy reflectivity parameters needs to be calibrated. Further studies are needed to explore these issues for the wide use of downward-scanning above-canopy lidar over large regions. Those issues can be investigated with data from an upward-scanning ground lidar like Echidna (Jupp et al., 2005).

The Echidna Validation Instrument (EVI), developed by CSIRO Australia as part of its canopy lidar initiative, is a ground-based, upward hemispherical-scanning, full waveform digitized, terrestrial lidar instrument and allows acquisition of vegetation canopy structure data, including height, basal area, stem counts, and branching parameters, as well as accurate information on standing woody and nonwoody biomass with height and related measures for carbon balance inventory and mapping (Jupp and Lovell, 2004; Jupp et al., 2005; 2008). EVI-measured vegetation structure data can then be integrated with downward-looking airborne lidar, such as LVIS, to map vegetation structure and carbon-balance parameters over large areas. The data also provide the opportunity for scaling up to regional and global levels; for example, using transects of the Geoscience Laser Altimeter System (GLAS) acquired by ICESat. To further explore the integration, EVI under-canopy hemispherical lidar scans have been obtained at North American test sites where LVIS and GLAS data have been acquired. This provides us an opportunity to analyze spatially coincident lidar waveforms acquired by the three sensor systems at their fine to coarse spatial resolutions, to calibrate LVIS from Echidna, and GLAS from Echidna and LVIS, and finally to map vegetation structure and carbon-balance parameters at LVIS and GLAS resolutions based on Echidna measurements.

The integration of below- and above-canopy lidar data will be supported by a consistent theoretical framework centered on the geometric optical and radiative transfer (GORT) model of canopy reflectance (Ni et al., 1997), which has its roots in the geometric-optical reflectance models (Li and Strahler,1985; 1986; 1988; 1992; Li et al., 1995; Strahler and Jupp, 1990). Use of a common modeling framework for lidar waveforms at ground, airborne, and spaceborne levels will facilitate integration and scaling of the data to provide large-area maps and inventories of vegetation structure and carbon stocks. It will also provide a pathway to refine the use of optical sensors that acquire multiangle imagery, such as the Multi-angle Imaging Spectroradiometer (MISR) and the Moderate Resolution Imaging Spectroradiometer (MODIS), to retrieve canopy structure in conjunction with lidars such as GLAS.

The GORT model was developed to describe the effects of three-dimensional (3D) canopy structure on the radiation environment and to characterize the heterogeneous radiation environment in natural vegetation at the forest stand scale (Li et al., 1995). Merging theory from geometric optics and radiative transfer, the GORT model treats vegetation canopies as assemblages of randomly distributed tree crowns of ellipsoidal shape. The tree crowns are filled with leaves that absorb and scatter radiation passing through the crown. Principles of radiative transfer are used in describing the multiple scattering of leaves inside crowns and the multiple scattering among crowns and the ground surface. The GORT model has been used successfully in describing the bidirectional reflectance distribution function (BRDF) characteristics of forests, including the "hotspot," and was extended by Ni et al. (1997) to include the vertical canopy gap probability profile.

Over time, GORT has proven very useful in a variety of applications. It has been successfully used to model photosynthetically active radiation (PAR) transmission, solar radiation transmission, and absorption by canopy elements in conifer forests (Ni et al., 1997), bidirectional reflectance (Ni et al., 1999a; Ni and Li, 2000), surface albedo (Ni and Woodcock,

2000), and spatial variance of remotely sensed images over vegetated land surfaces (Ni et al., 1999b; Ni and Jupp, 2000). Song and Woodcock (2002; 2003) and Song et al. (2002) used the GORT model successfully to model the reflectance of Oregon forest stands as a function of age or successional stage as well as observed effects of topography and view angle on optical imagery.

GORT has also been successfully applied to model airborne vegetation lidar waveforms as a function of vegetation structure parameters such as tree size, height, and density, and foliage volume density (Ni-Meister et al., 2001). It also deals with multilayer and multispecies vegetation canopies through convolution of mixed communities (Ni-Meister et al., 2001). The purpose of this study is to apply the GORT model to study the link between the below-canopy EVI signals and the vegetation structure parameters. The current GORT model will be extended to include the effect of trunks on EVI signals in a single layer and will be further evaluated in a multilayered vegetation canopy. The modeled gap probability profiles will be compared with EVI-derived canopy gap probability profiles in a one-layer pine plantation and a two-layer eucalypt natural forest near the Tumbarumba flux tower site, New South Wales, Australia.

Extended leaf-and-trunk GORT model

One important concept used to quantify the effect of the 3D vegetation structure on the radiation environment within canopies and lidar returns is the directional canopy gap probability, or the probability that a photon from one particular incident angle will reach a point at a certain height in the canopy without being scattered. The directional gap probability is a fundamental quantity modeled by GORT and is used to build the bridge between the canopy structure parameters that drive GORT and the return lidar waveforms measured from Echidna, LVIS, and GLAS (Ni-Meister et al., 2001; Lovell et al., 2003; Jupp and Lovell, 2004; Jupp et al. 2008). The basic lidar equation linking the canopy gap probability with lidar return has been fully discussed in previous papers. In particular, Jupp et al. (2008) give a detailed description of how to derive the canopy gap probability from below-canopy upward-scanning lidar measurements. In this study, we evaluate the GORT model by comparing the GORT-modeled and EVI-derived gap probability profiles. The following describes the gap probability part of the GORT model.

The original leaf GORT model for lidar

The GORT model was developed to describe the effects of 3D canopy structure parameters of discrete canopies on the radiation environment and to characterize the radiation environment in natural vegetation at the forest stand scale, based on the theories of geometric optics and radiative transfer. For the vegetation lidar application, we only use the canopy gap probability part of the full GORT model, which is similar to other types of canopy gap probability models (Nilson, 1999). In the GORT model, a discontinuous canopy layer is modeled as an assemblage of randomly distributed tree crowns of ellipsoidal shape, having horizontal crown radius R and vertical crown radius b, and centered between heights h_1 and h_2, where h_1 and h_2 are the lower and upper bounds of crown center heights, respectively. Within each single crown, the foliage and branches are assumed to be uniformly distributed. The primary vegetation structure parameters driving GORT are tree density (stems per hectare), tree size and shape, foliage density, and the upper and lower bounds of crown center height.

In the original leaf GORT model, the penetration of laser beams is described by the summation of two types of gap probabilities: the between-crown gap probability, $P_{\text{crn}}(n = 0 \mid \theta, z)$, and the within-crown gap probability, $P_{\text{crn}}(n > 0 \mid \theta, z)$. When laser beams pass through the canopy layer, some proportion will pass through the canopy without passing through tree crowns (referred to as between-crown gap probability), while another proportion may pass through crowns without being scattered (within-crown gap probability). The between-crown gap probability, $P_{\text{crn}}(n = 0 \mid \theta, z)$, for laser beams describes the proportion of the laser beams at incident angle θ that reaches a point located at height z without passing through any crowns (i.e., $n = 0$). This is the probability that there are no crown centers within the beam-projected cylinder volume with a radius R starting from the incident canopy layer to height z, otherwise the beam will pass through crowns. Based on Boolean theory (Serra, 1982), the between-crown gap probability is expressed as an exponential function of crown projected volume in the laser incident angle. The within-crown gap probability, $P_{\text{crn}}(n > 0 \mid \theta, z)$, is defined as the proportion of laser beams passing through at least one crown without being scattered. The calculation of the within-crown gap probability can be described by Beer's law, assuming the canopy elements are much smaller than the crown envelopes, where the within-crown pathlength is dependent on the location where a beam enters a crown, the number of crowns through which it passes, and the pathlength through an individual crown (see the details in Li et al. (1995) and Ni et al. (1997)). Canopy gap probability is modeled as a function of vegetation geometry parameters, including tree size, shape, and density, and foliage volume density.

The original GORT model treats all woody components as random scatters, like leaves. As a result, the original GORT model can be considered a "leaf model." In some special cases, such as in winter, GORT has been used to estimate the radiation environment in leaf-off forests (Hardy et al., 1998). In this situation, trunks and branches are simply treated as randomly distributed "leaves" within crowns, and foliage volume density is replaced by stem area volume density in the model. However, when modeling the return from below-canopy lidars, a more rigorous treatment of the trunks is necessary. In the following section, the original "leaf-only" GORT is extended to include both leaves and trunks.

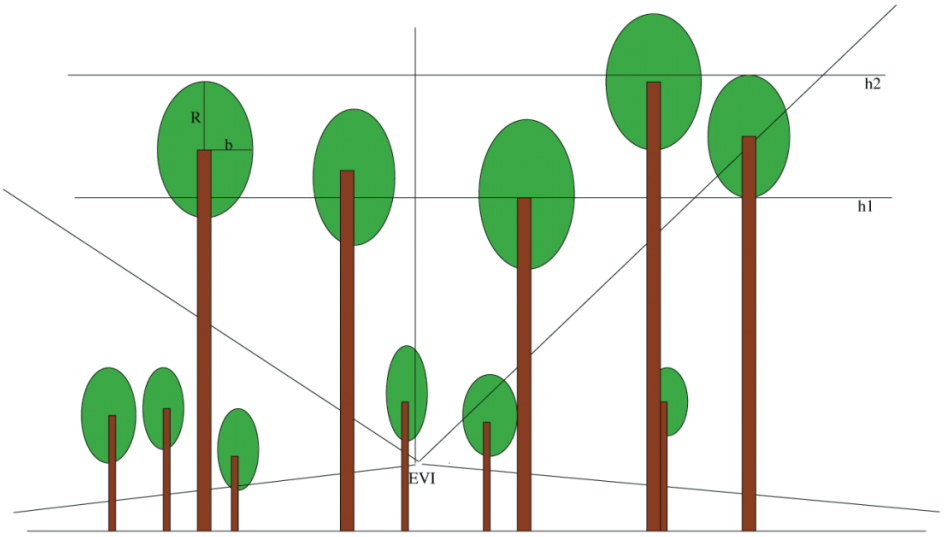

Figure 1. Extended multilayered trunk-and-leaf/stem geometric-optical and radiative-transfer (GORT) model used to model the ground-based upward-looking lidar EVI-measured gap probabilities.

The extended leaf-and-trunk GORT model

In the original GORT model of lidar, the incident radiation is from above the canopy. For below-canopy lidar, laser beams enter the canopy from the bottom of the canopy, and the gap probability decreases with height. Since the canopy layer is modeled as symmetric, the gap probability modeled by the leaf GORT model can be flipped and applied for modeling below-canopy lidar returns.

Figure 1 illustrates the scene model of the leaf-and-trunk GORT model as well as the sensing scenario of the EVI. In the leaf-and-trunk GORT model, vegetation canopies are modeled as assemblages of randomly distributed tree crowns of ellipsoidal shape. The trunks are treated as randomly distributed cylinders with the diameter of DBH and the height of the crown center height (see **Figure 1**). The addition of trunks to the model requires the additional input of diameter at breast height (dbh), above and beyond the normal requirements for tree size (horizontal (R) and vertical (b) crown radii), lower and upper crown center heights (h_1 and h_2), tree density (λ), and foliage volume density (F_a) used in the leaf GORT model.

The total gap probability is the sum of the between-crown/trunk and within-crown gap probability. The between-crown/trunk gap probability is the product of between-crown, $P_{\text{crn}}(n=0\,|\,\theta,z)$, and between-trunk, $P_{\text{trk}}(n=0\,|\,\theta,z)$, gap probabilities. Between-crown, $P_{\text{crn}}(n=0\,|\,\theta,z)$, and within-crown, $P_{\text{crn}}(n>0\,|\,\theta,z)$, gap probabilities are calculated in the same way as in the original leaf GORT model (Ni et al.,1997). Based on geometric optics, the between-trunk gap probability, $P_{\text{trk}}(n=0\,|\,\theta,z)$, is calculated as an exponential function of the projected trunk volume, in a similar way as in the between-crown gap probability. The projected trunk volume is a function of DBH and tree height. The difference in canopy gap probability profiles modeled by the leaf GORT and leaf-and-trunk GORT can be listed as follows:

Leaf GORT: $$P(\theta,z)=P_{\text{crn}}(n=0\,|\,\theta,z)+P_{\text{crn}}(n>0\,|\,\theta,z)$$

Leaf-and-truck GORT: $$P(\theta,z)=P_{\text{crn}}(n=0\,|\,\theta,z)P_{\text{trk}}(n=0\,|\,\theta,z)+P_{\text{crn}}(n>0\,|\,\theta,z)$$

To demonstrate the difference between leaf GORT and leaf-and-trunk GORT models, **Figure 2** shows the comparison of the modeled between-trunk, between-crown, within-crown, and the total gap probabilities from leaf GORT and leaf-and-trunk GORT in a one-layer pine plantation at two different zenith rings (incident zenith angles). The projected trunk volume increases linearly with height and keeps constant above the crown center height. The between-trunk gap probability decreases exponentially with height and keeps constant above the height of the crown centers. Thus, the effect of trunks on the between-trunk gap probability increases with height.

However, the effect of trunks on the total gap probability, shown in **Figure 2** as the difference of total gap probabilities from the leaf GORT and the leaf-and-trunk GORT, increases and then decreases with height. Below the canopy layer, the only gap is between trunks, and the effect of trunks on the gap probability increases and reaches its largest effect in the lower part of the canopy, and then decreases with height. The main reason for an insignificant trunk effect on the total gap probability in the upper part of the canopy layer is that the trunk effect is multiplied by the between-crown gap probability, which decreases with height. **Figure 2** also shows that the trunk effect on the total gap probability increases with incident zenith rings, indicating that at large incident zenith rings, laser beams from the EVI hit more trunks. In summary, the effect of trunks on the total gap probability for a single-layer canopy is strong

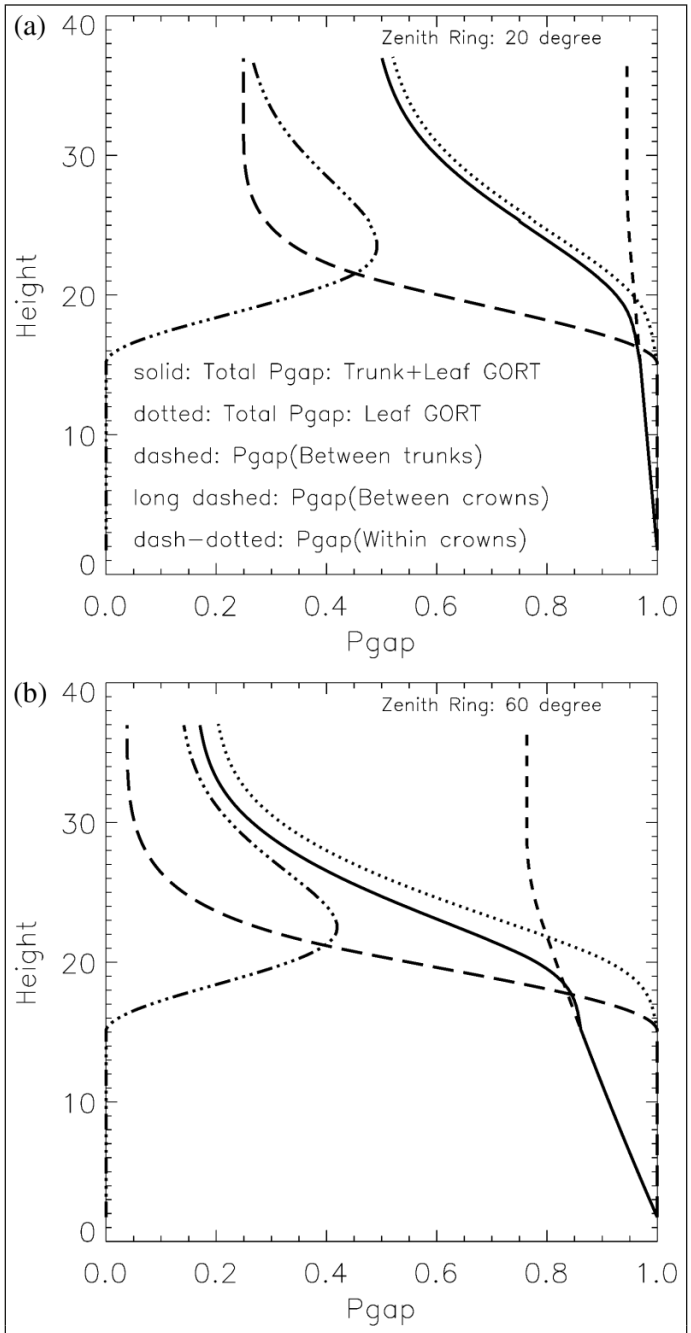

Figure 2. Modeled gap probabilities for different zenith ranges using the leaf-only and leaf-and-trunk geometric-optical radiative-transfer (GORT) models in the pine plantation near the Tumbarumba flux tower site, New South Wales, Australia. Between-crowns, within-crowns, and between-truck gap probabilities are also shown.

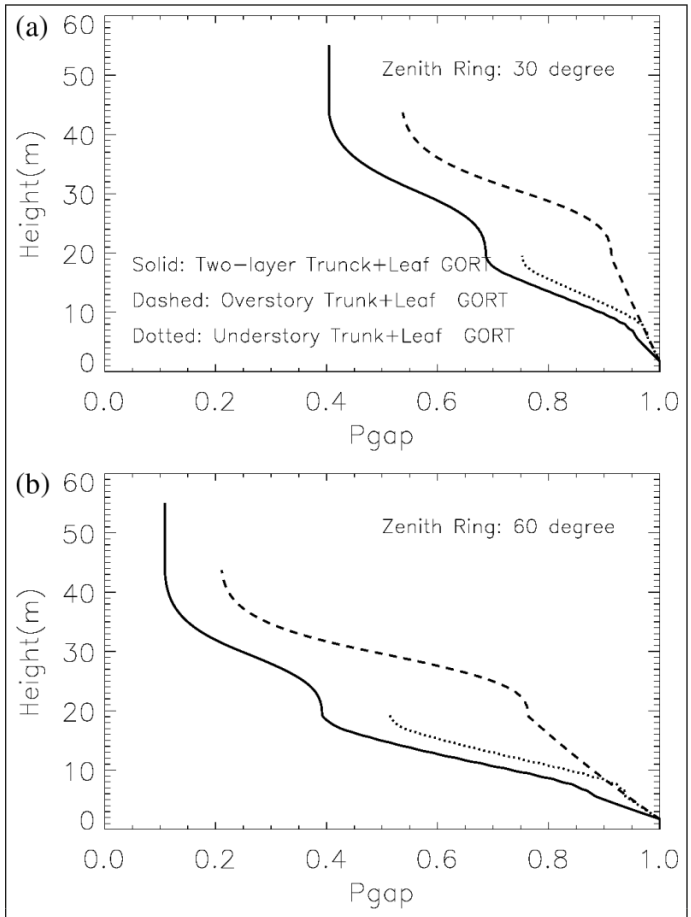

Figure 3. Modeled gap probabilities for two different zenith ranges for a single layer (overstory and understory) overlayed with a two-layer eucalypt forest near the Tumbarumba flux tower site, New South Wales, Australia.

below and in the lower part of the canopy, and the trunk effect is larger at larger zenith rings.

The multilayered GORT model

Forest canopies often occur in layers as a result of mixes of species and (or) ages of trees (see **Figure 1**). To calculate gap profiles for multilayered canopies, the gap probability for each single layer is calculated first, and the total gap probability is obtained by convoluting the gap probability profile for each canopy layer.

To demonstrate the difference in canopy gap probability profiles for one- and two-layer canopies, **Figure 3** shows the modeled total gap probability in a two-layer eucalypt forest in Australia together with gap probability profiles for the two individual canopy layers at two different zenith rings. **Figure 3** demonstrates that by using only one layer, the leaf-and-trunk GORT model results in large overestimation of the canopy gap probability.

To further illustrate the effect of trunks on the canopy gap probability for a two-layer canopy, **Figure 4** shows the comparison of total gap probability profiles in the two-layer eucalypt forest, modeled using both the leaf and the leaf-and-trunk GORT models. The effect of trunks on the gap probability is the difference of the two gap probability profiles in **Figure 4**, and increases with the incident zenith rings. The largest effect is in the middle lower part of the upper canopy layer between about 15 and 25 m. The trunk effect is also strong in the upper part of the upper canopy layer, which is different from the single-layer case. This is due to the fact that the two-layer gap

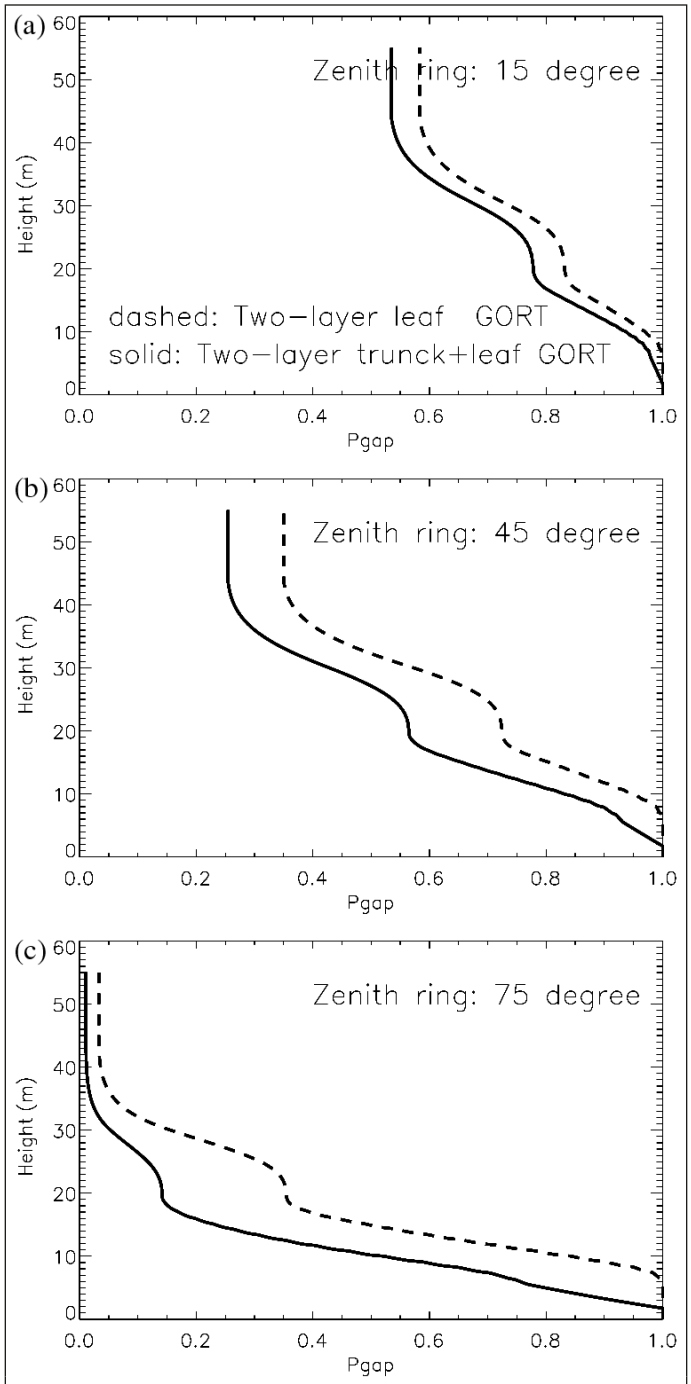

Figure 4. Modeled gap probabilities for two different zenith ranges for the leaf-only (dashed lines) and the leaf-and-trunk (solid lines) geometric-optical radiative-transfer (GORT) models in a two-layer eucalypt forest near the Tumbarumba flux tower site, New South Wales, Australia.

probability is the convolution of the gap probabilities of the two layers. The trunk effect in each layer is convoluted and propagated to the total gap probability profiles, resulting in large differences in the total probability profiles when trunks are added. This overall trunk effect in a two-layer canopy is different from the trunk effect in a single-layer canopy. Interestingly, the effect of trunks on a two-layer canopy not only influences the lower canopy layer, but the upper layer as well. The effects are the strongest in the lower part of the upper canopy layer and increase with the zenith angle.

Model evaluation

Site description

Our study sites include a pine plantation (ponderosa pine) near the Tumbarumba flux tower site, (referred to as the "pine site" in this study) and a native tall eucalypt forest at the Tumbarumba flux tower site (referred to as the "tower site") in southeastern New South Wales, Australia. The pine site is a uniform plantation without extensive understory. The eucalypt forest has an average tree height of roughly 40 m and the canopy is roughly divided into two layers. There is also significant ground cover of shrubs and grasses (see Strahler et al., 2008; this issue) for details).

Field measurements and model parameterization

One EVI scan was acquired in the pine site and eight EVI scans were collected in eight plots in the eucalypt forest in a square arranged around the Tumbarumba flux tower in November 2006 (Jupp et al., 2008; Strahler et al., 2008). The eight scans are tower east (ee), tower northeast (ne), tower north (nn), tower northwest (nw), tower southeast (se), tower south (ss), tower southwest (sw), tower west (ww). EVI data were processed to generate gap probabilities at different zenith ring ranges based on the method described in Jupp et al. (2008). In this study, we compared the modeled and EVI-measured gap probabilities to evaluate the model performance.

The required parameters for the GORT model were measured in the field or extracted from the literature. At the pine site, the location and dbh of each tree in a 50 m radius plot were recorded. At the eight tower sites, variable radius plots were collected at each point using a 2 m^2/ha basal area factor. For these sites, the location, species, and dbh of each "in" tree were recorded. Four trees in the pine site and 31 trees in the tower site were sampled to measure the relationship between dbh and tree height and crown geometry (horizontal and vertical crown radii), tree height. The tree density for the pine site is simply the number of trees divided by the area of the plot. For the variable radius plots, conventional density expansions were used. The pine site was treated as a one-layer canopy and the tower site as a two-layer canopy. The upper and lower layers were distinguished by the canopy position, as recorded in the field: *I* (intermediate) was treated as lower layer trees and and *D*/*C* (domainal/co-domainal) as upper layer trees.

GORT inputs, except h_1 and h_2, were parameterized from the above measurements (**Table 1**). Tree size and density were calculated as mean values of all measured trees for the pine site, but were weighted by the basal area for the tower site. For each individual plot in the tower site, tree geometry parameters were calculated based on DBH to increase the samples. Foliage

Table 1. Input tree geometry parameters in three sites.

Site	R (m)	$\frac{b}{R}$	λ (tree/m^{-2})	F_a (m^2/m^3)	h_1 (m)	h_2 (m)	dbh (m)	LAI
Pine	5.7	1.41	0.012	0.19	23.15	29	0.53	2.5
Tower_underlayer	0.972	1.614	0.066	2.2	6.99	17.91	0.146	0.9
Tower_upperlayer	3.325	2.038	0.013	0.35	25.66	36.89	0.694	1.43

volume density (F_a) was calculated from the leaf area index (LAI), tree size, and density measurements, based on the following formula:

$$F_a = \frac{\text{LAI}}{\frac{4}{3}\lambda\pi R^2 b}$$

The LAI values were obtained from Leuning et al. (2005). The values for h_1 and h_2 were obtained based on EVI waveform measurements through visualization. Based on the inputs described above, gap probability profiles for the pine and tower sites were modeled using the leaf and the leaf-and-trunk GORT models and compared with EVI-derived gap probability profiles.

Modeled and EVI-measured gap probability comparison

Gap probability comparison at the pine site

As described above, all GORT input parameters are stand averages. Thus, the GORT-modeled gap probability represents canopy gap probabilities over a region/stand. **Figure 5** shows the EVI-derived mean gap probability profiles at different ranges of zenith rings (row 1: 0–5°; row 2: 15°; and row 4: 20° ranges). The purpose of the averaging process is to increase the sampling area. The size of the solid angle of laser beam of EVI varies 2–15 mrad. The averaged waveform/gap probability within 5° zenith rings corresponds roughly to the volume difference between two cones, which is (1/3)*pi*(20 m)^3*(sin(θ + 5)^2*cos(θ + 5) – sin(θ)^2*cos(θ)) at a 20 m distance range. The sampling size increases with the incident zenith angle. **Figure 5** shows the following three features. First, at smaller zenith rings, laser beams impact a relatively small local area and the EVI-derived gap probability does not show a smooth decrease with the increase of zenith rings. However, when averaging with a 20° range, the EVI gap probability does show a smooth decrease with the zenith rings, indicating that the gap probability represents the statistical canopy structure characteristics. Second, at relatively large zenith rings, averaging the gap probability at different zenith rings does not affect the gap probability, indicating that laser beams impact relatively larger areas, even for a 5° zenith range. Lastly, gap probability profiles in the lower part of the canopy decrease with incident zenith rings, indicating a strong trunk effect on gap probability profiles at large zenith rings. The above features indicate that it is reasonable to compare GORT-modeled values with the mean EVI gap probability within a 20° zenith range.

Figure 6 shows the comparison of leaf GORT- and leaf-and-trunk GORT-modeled and averaged EVI-derived gap probability profiles within a 20° zenith range for different zenith rings. The leaf-and-trunk GORT-modeled gap profiles match better with the EVI gap probability profiles than the leaf GORT-modeled gap profiles, particularly at large zenith rings. The leaf-and-trunk GORT-modeled gap probability profiles in the lower part of the canopy matched very well with EVI-measured ones, indicating that the extended leaf-and-trunk GORT model is able to model the effect of woody structures on EVI measurements at the pine site.

Gap probability comparison at the tower site

EVI gap probabilities at the eight tower sites were averaged to produce the averaged gap probability at different ranges of zenith rings, and the same procedure was used to average EVI gap probabilities at different zenith ranges (**Figure 7**). Compared with the EVI gap probability at the pine site, the averaged EVI gap probability profile at the eight sampling points shows a similar changing pattern with incident zenith ring ranges and decreases with zenith rings. Those patterns indicate that the eight-point averaged EVI gap probability profiles, even at 5° zenith range, represent the averaged canopy gap probability at a stand scale and is comparable to the GORT-modeled gap probability. The EVI-derived gap probability at each site was also included in Figure 7 to show the spatial variations. The variation of gap probability varies with zenith rings, with larger variations at smaller zenith rings. A large variation in different plots at small zenith ring is governed by the large variation of the sample areas, as discussed before.

Figure 8 shows the comparison of the mean and standard deviation of the modeled and EVI canopy gap probability profiles at every 5° zenith range in the tower site. Overall, the leaf-and-trunk GORT-modeled gap probability matches better with the EVI gap probability profiles at different angles than the leaf-only GORT model. Ignoring the effect of trunks, the leaf GORT-modeled gap probability overestimates the EVI gap probability. However, the modeled gap probability profile shows a bump in the lower part of the upper canopy layer. One reason may be the fact that the overlay layer used in the model, which is represented by the difference of the lower boundary of the upper canopy layer and the upper boundary of the lower canopy layer, is too thin. A better strategy may be necessary to parameterize these two sets of parameters. Another reason might be the effect of ignoring the large understory in the foliage density parameterization in the lower canopy layer. However, overall, the leaf-and-trunk GORT-modeled gap

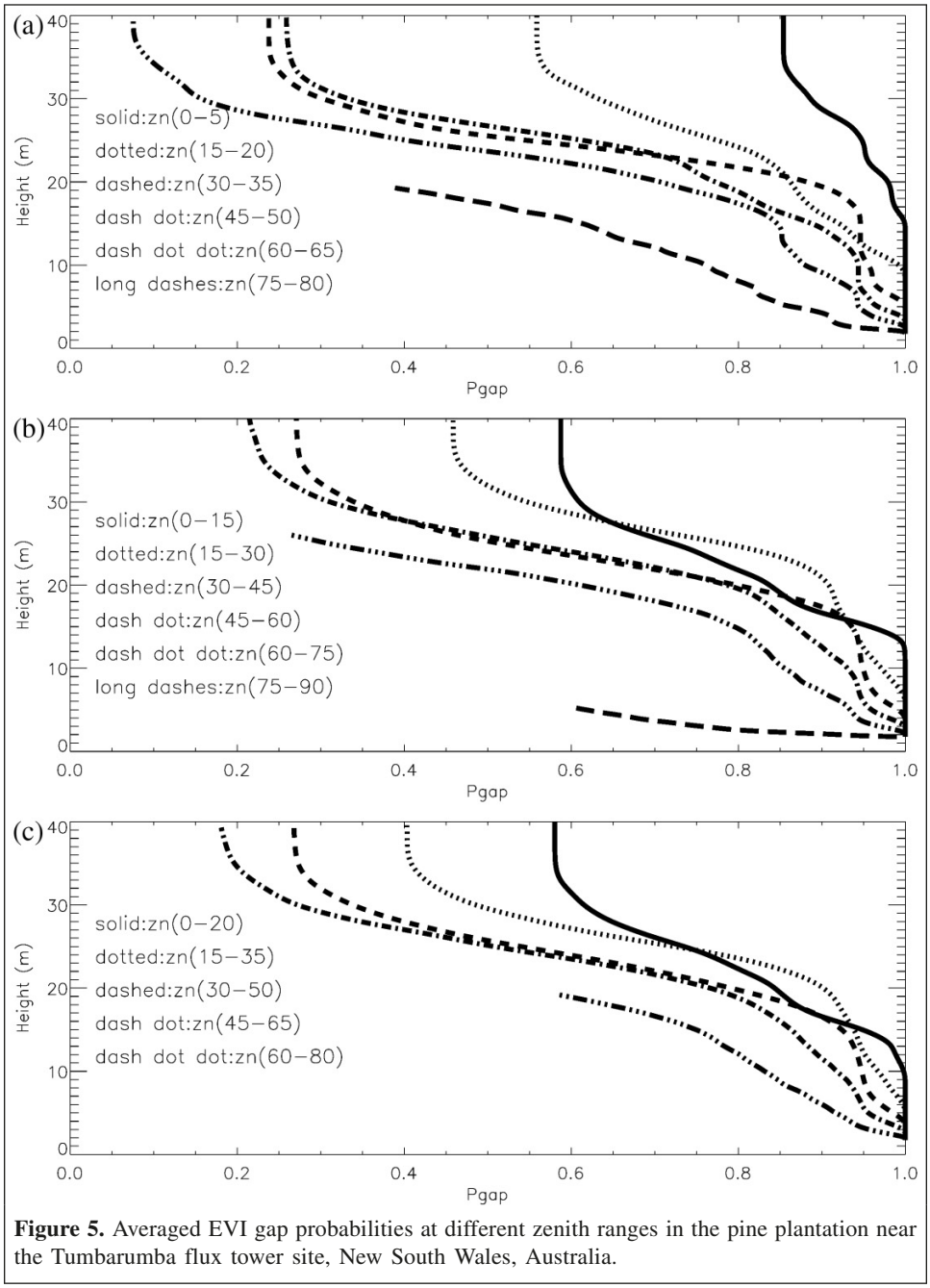

Figure 5. Averaged EVI gap probabilities at different zenith ranges in the pine plantation near the Tumbarumba flux tower site, New South Wales, Australia.

probability matches well with the EVI-measured canopy gap probability profiles, and using leaf-only GORT overestimates the canopy gap probability in the two-layer canopy.

Figures 6 and **8** do show a slight overestimation of the canopy gap probability by the model at small incident zenith rings such as 20°–35° (we ignore the very small rings, such as 0°–20°, which are underrepresented by the EVI sampling). This may be due to the effect of ignoring clumping when retrieving LAI values either from fisheye or LI-2000 measurements, leading to an underestimate of foliage area volume density. This overestimation indicates that the foliage area volume density parameter is a very sensitive parameter, and accurate input is required to best evaluate the performance of the GORT model.

The standard deviation from the model shows larger variations than the one from the EVI measurements at large zenith rings. Large uncertainties of the model input parameters contribute to the large variation of the modeled results. Within each plot, the tree size geometry parameters were derived from the sufficient DBH measurements available within each plot. A large variation in the model results also indicates that the GORT-modeled canopy gap probability is quite sensitive to model inputs. The use of averaged inputs for the whole tower site does not demonstrate this mismatched sampling issue.

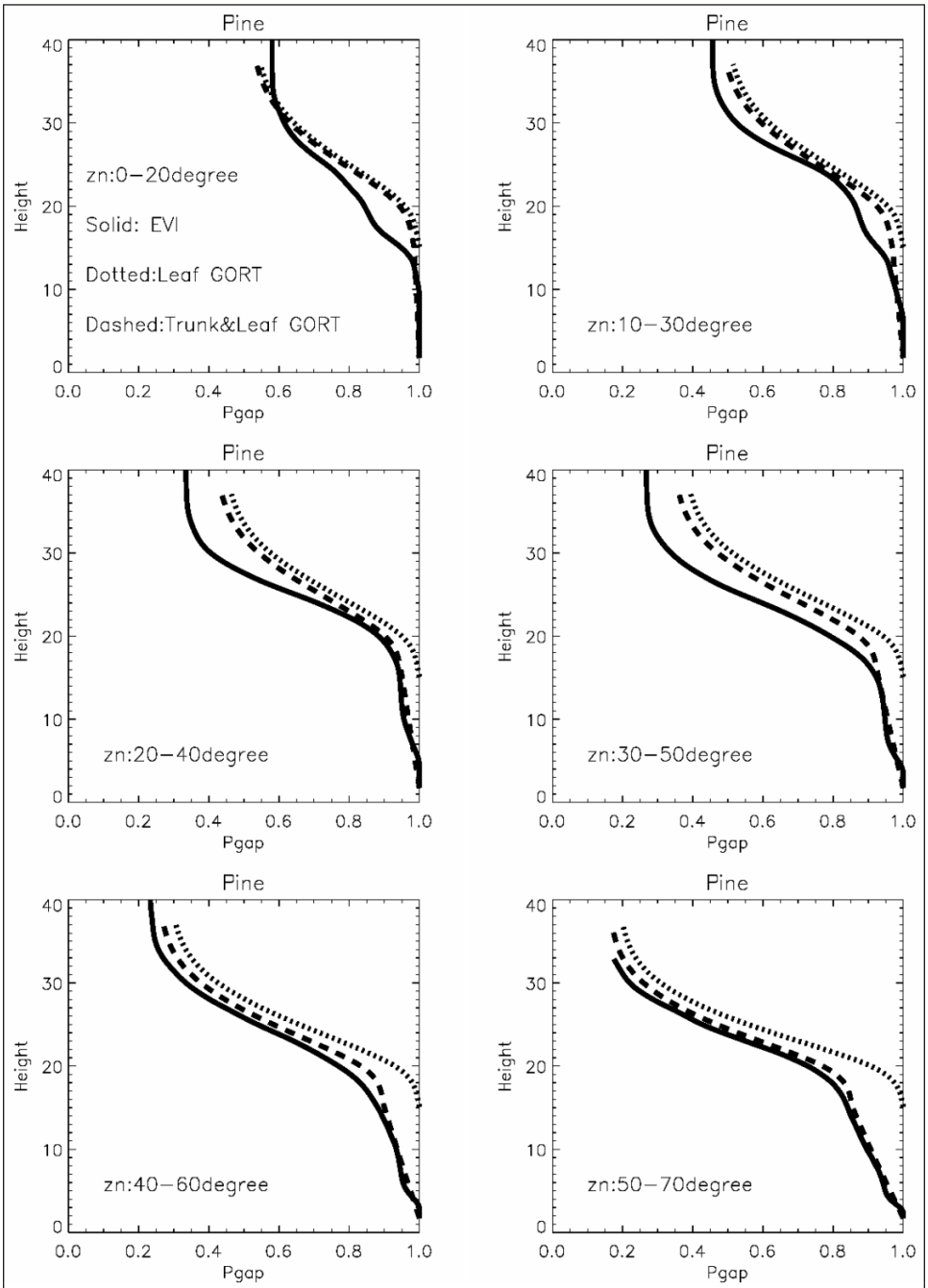

Figure 6. Comparison of the original (leaf only) GORT (blue), extended (leaf-and-trunk) GORT (red), and EVI-derived (black) canopy gap probabilities (P_{gap}) at a 20° zenith rings averaged angle in a one-layered pine plantation near the Tumbarumba flux tower site, New South Wales, Australia.

Discussion and conclusions

To apply the GORT model in the context of upward-looking below-canopy lidar measurements, it was necessary to extend the original "leaf" GORT model to include the effects of tree trunks. The extended GORT model was evaluated by comparing the modeled and EVI-derived gap probability profiles in a one-layer pine plantation and a two-layer eucalypt forest at the Tumbarumba flux tower site in southeastern New South Wales, Australia. The results show that the leaf-and-trunk GORT model better estimates canopy gap probability profiles (as measured with EVI) than the leaf GORT model in both the one-layer and two-layer vegetation canopies. The results show that EVI-derived canopy gap probability profiles are linked with vegetation structure parameters, including tree size, tree density, foliage volume density, and tree height values.

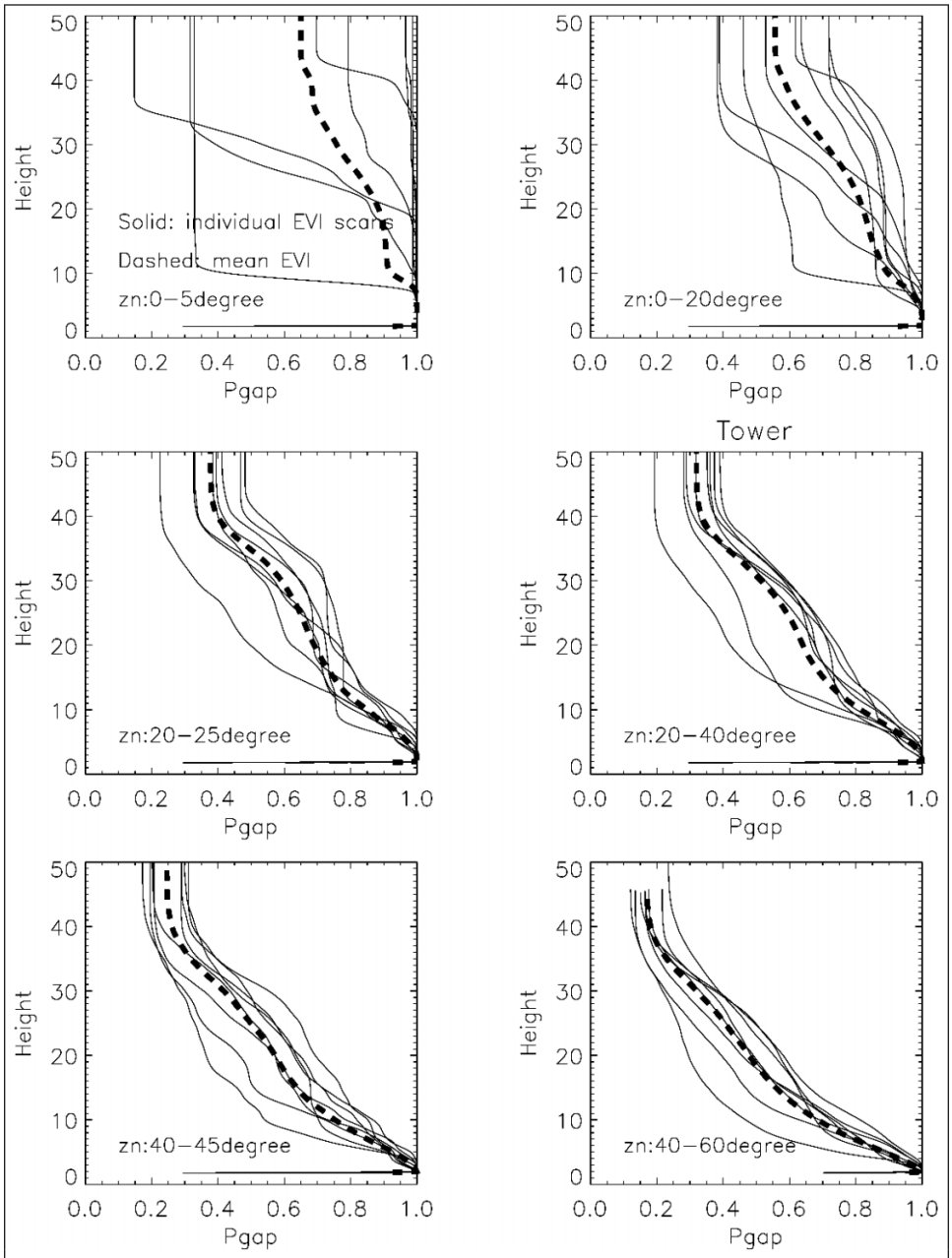

Figure 7. Averaged and individual EVI scan-derived gap probabilities at different zenith ranges in a two-layered eucalypt forest for eight sampling points in the Tumbarumba flux tower site, New South Wales, Australia.

This study demonstrates the utility of using gap probability profiles as a way to characterize forest canopy structure as they relate to lidar measurements. The ability to relate both above-canopy lidar measurements and below-canopy hemispherical lidar measurements through the same model, based on a common set of canopy parameters, is a key step toward an improved understanding of the information content of above-canopy lidars that should improve future efforts to retrieve forest canopy structural information, such as tree height, mean tree diameter, basal area, stem count density, crown diameter, woody biomass, and green biomass.

Use of a common model for lidar waveforms at the surface, airborne, and spaceborne levels provides exciting opportunities concerning the integration and scaling of these diverse data types to provide large-area maps and inventories of vegetation structure and carbon stores. By exploiting physical theory through GORT, we anticipate an improved ability to adapt and apply retrieval algorithms over large areas and to adjust algorithms to new surface conditions or sensing configurations. It would be possible, therefore, to predict changes in lidar waveforms as a function of view angle for specific combinations of canopy properties. Use of a common model

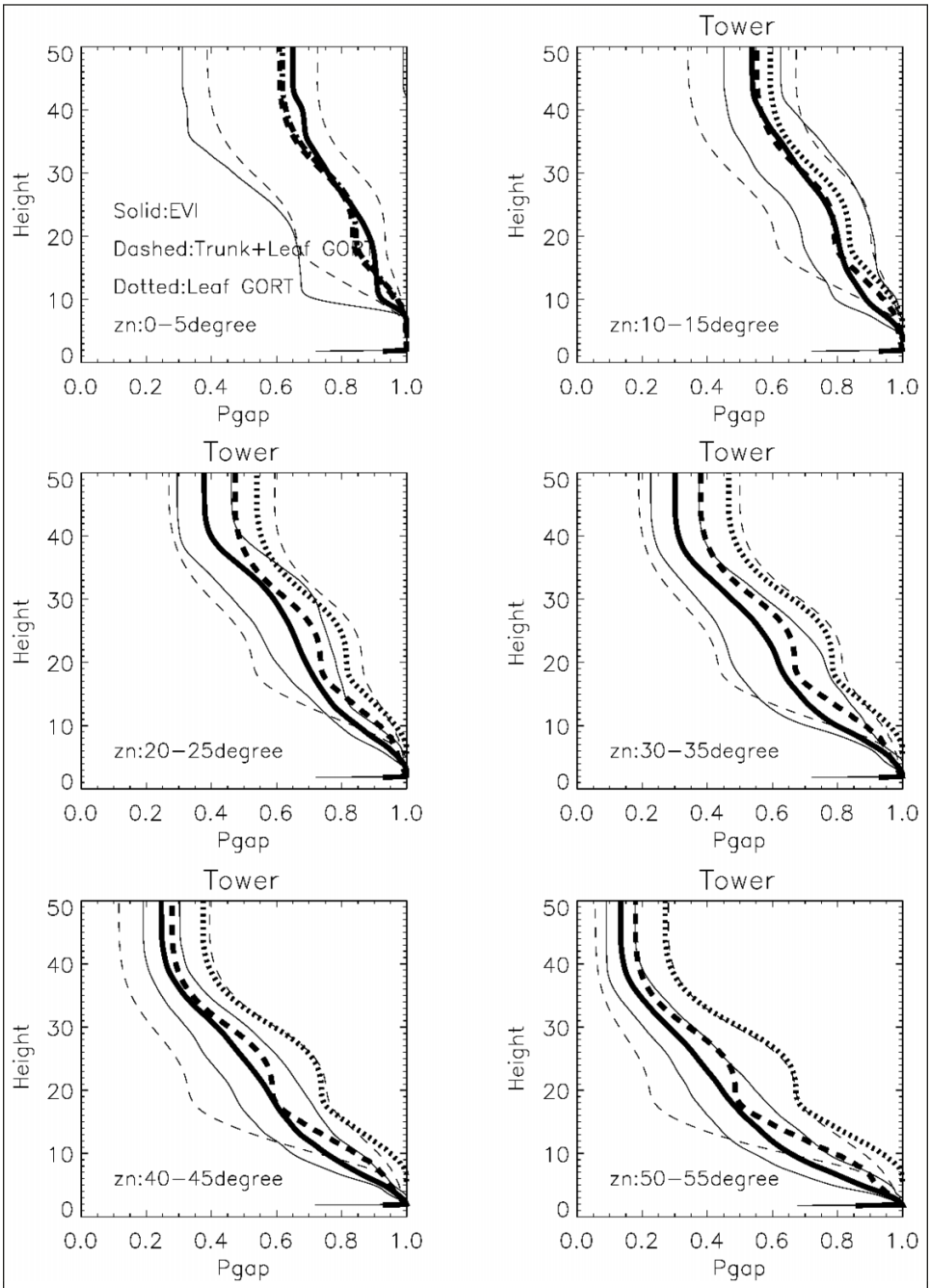

Figure 8. Comparison of original (leaf-only) GORT (dotted), extended (trunk-and-leaf) GORT (dashed), and EVI-derived (solid) canopy gap probabilities (P_{gap}) with standard deviations (thin dashed line for trunk-and-leaf GORT and solid lines for EVI) at a 5° zenith rings averaged angle in a two-layer eucalypt forest in the Tumbarumba flux tower site, New South Wales, Australia. The extended GORT is able to capture the characteristics of P_{gap} from both leaf and trunks in a two-layered canopy.

will facilitate the scaling of small-footprint full waveform digitized lidar to large-footprint airborne or spaceborne lidar and the study of future lidar mission requirements. Future work, therefore, will explore the linkage of ground-based lidar with large-footprint airborne (LVIS) and spaceborne vegetation lidar data (GLAS).

Acknowledgements

This work was funded by NASA under grant NNG06GI92G. Thanks are due for the support from CSIRO Marine and Atmospheric Research and CSIRO Forest Biosciences. Special thanks go to the two anonymous reviewers for their time and effort in reviewing this paper.

References

Blair, J.B., Rabine, D.L., and Hofton, M.A. 1999. The Laser Vegetation Imaging Sensor: a medium-altitude, digitisation-only, airborne laser altimeter for mapping vegetation and topography. *ISPRS Journal of Photogrammetry and Remote Sensing*, Vol. 54, Nos. 2–3, pp. 115–122.

Drake, J.B., Dubayah, R.O., Clark, D.B., Knox, R.G., Blair, J.B., Hofton, M.A., et al. 2002a. Estimation of tropical forest structural characteristics using large-footprint lidar. *Remote Sensing of Environment*, Vol. 79, Nos. 2–3, pp. 305–319.

Drake, J.B., Dubayah, R.O., Knox, R.G., Clark, D.B., and Blair, J.B. 2002b. Sensitivity of large-footprint lidar to canopy structure and biomass in a neotropical rainforest. *Remote Sensing of Environment*, Vol. 81, Nos. 2–3, pp. 378–392.

Drake, J.B., Knox, R.G., Dubayah, R.O., Clark, D.B., Condit, R., Blair, J.B., and Hofton, M. 2003. Above-ground biomass estimation in closed canopy neotropical forests using lidar remote sensing: factors affecting the generality of relationships. *Global Ecology and Biogeography*, Vol. 12, No. 2, pp. 147–159.

Dubayah, R.O., and Drake, J.B. 2000. Lidar remote sensing for forestry. *Journal of Forestry*, Vol. 98, No. 6, pp. 44–46.

Harding, D.J., and Carabajal, C.C. 2005. ICESat waveform measurements of within-footprint topographic relief and vegetation vertical structure, *Geophysical Research Letters*, Vol. 32, L21S10, doi:10.1029/2005GL023471.

Harding, D.J., Lefsky, M.A., Parker, G.G., and Blair, J.B. 2001. Laser altimeter canopy height profiles – methods and validation for closed-canopy, broadleaf forests. *Remote Sensing of Environment*, Vol. 76, No. 3, pp. 283–297.

Hardy, J.P., Davis, R.E., Jordan, R., Ni, W., and Woodcock, C.E. 1998. Snow ablation modeling in conifer and deciduous stands of the boreal forest, *Hydrological Processes*, Vol. 12, pp. 1763–1778.

Jupp, D.L.B., and Lovell, J. 2004. Product background and description for airborne (VSIS) and ground-based (Echidna®) canopy lidar systems. Canberra, ACT, Australia, CSIRO Earth Observation Centre.

Jupp, D.L.B., Culvenor, D.S., Lovell, J., and Newnham, G. 2005. Evaluation and validation of canopy laser radar (lidar) systems for native and plantation forest inventory. Canberra, ACT, Australia, CSIRO Earth Observation Centre and CSIRO Forestry and Forest Products Division. 150 pp.

Jupp, D.L.B., Culvenor, D.S., Lovell, J., and Newnham, G. 2007. Estimating forest LAI profiles and structural parameters using a ground based laser called "Echidna®". *Tree Physiology,* In Press.

Lefsky, M.A., Cohen, W.B., Acker, S.A., Parker, G.G., Spies, T.A., and Harding, D. 1999. Lidar remote sensing of the canopy structure and biophysical properties of Douglas-fir western hemlock forests. *Remote Sensing of Environment*, Vol. 70, No. 3, pp. 339–361.

Lefsky, M.A., Cohen, W.B., Parker, G.G., and Harding, D.J. 2002. Lidar remote sensing for ecosystem. *Bioscience*, Vol. 52, No. 1, pp. 19–30.

Lefsky, M.A., Harding, D.J., Keller, M., Cohen, W.B., Carabajal, C.C., Espirito-Santo, F.D.B., et al. 2005. Estimates of forest canopy height and aboveground biomass using ICESat. *Geophysical Research Letters*, Vol. 32, L22S02, doi:10.1029/2005GL023971.

Leuning, R., Cleugh, H.A., Zegelin, S.J., and Hughes, D. 2005. Carbon and water fluxes over a temperate Eucalyptus forest and a tropical wet/dry savanna in Australia: measurements and comparison with MODIS remote sensing estimates. *Agricultural and Forest Meteorology*, Vol. 129, pp. 151–173.

Li, X., and Strahler, A.H. 1985. Geometric-optical modeling of a conifer forest canopy. *IEEE Transactions on Geoscience and Remote Sensing*, Vol. GE-23, No. 5, pp. 705–721.

Li, X., and Strahler, A.H. 1986. Geometric-optical bidirectional reflectance modeling of a conifer forest canopy. *IEEE Transactions on Geoscience and Remote Sensing*, Vol. GE-24, No. 6, pp. 906–919.

Li, X., and Strahler, A.H. 1988. Modeling the gap probability of a discontinuous vegetation canopy. *IEEE Transactions on Geoscience and Remote Sensing*, Vol. 26, No. 2, pp. 161–170.

Li, X., and Strahler, A.H. 1992. Geometric-optical bidirectional reflectance modeling of the discrete crown vegetation canopy – effect of crown shape and mutual shadowing. *IEEE Transactions on Geoscience and Remote Sensing*, Vol. 30, No. 2, pp. 276–292.

Li, X., Strahler, A.H., and Woodcock, C.E. 1995. A hybrid geometric optical-radiative transfer approach for modeling albedo and directional reflectance of discontinuous canopies. *IEEE Transactions on Geoscience and Remote Sensing*, Vol. 33, No. 2, pp. 466–480.

Lovell, J.L., Jupp, D.L.B., Culvenor, D.S., and Coops, N.C. 2003. Using airborne and ground-based ranging lidar to measure canopy structure in Australian forests. *Canadian Journal of Remote Sensing*, Vol. 29, No. 5, pp. 607–622.

Means, J.E., Acker, S.A., Harding, D.J., Blair, J.B., Lefsky, M.A., Cohen, W.B., et al. 1999. Use of large-footprint scanning airborne lidar to estimate forest stand characteristics in the Western Cascades of Oregon. *Remote Sensing of Environment*, Vol. 67, No. 3, pp. 298–308.

Nelson, R., Krabill, W., and MacLean, G. 1984. Determining forest canopy characteristics using airborne laser data. *Remote Sensing of Environment*, Vol. 15, No. 3, pp. 201–212.

Nelson, R., Valenti, M.A., Short, A., and Keller, C. 2003. A multiple resource inventory of Delaware using airborne laser data. *Bioscience*, Vol. 53, No. 10, pp. 981–992.

Ni, W., and Jupp, D.L.B. 2000. Spatial variance in directional remote sensing imagery—recent developments and future perspectives. *Remote Sensing Reviews*, Vol. 18, Nos. 2–4, pp. 441–479.

Ni, W., and Li, X.W. 2000. A coupled vegetation-soil bidirectional reflectance model for a semiarid landscape. *Remote Sensing of Environment*, Vol. 74, No. 1, pp. 113–124.

Ni, W., and Woodcock, C.E. 2000. Effect of canopy structure and the presence of snow on the albedo of boreal conifer forests. *Journal of Geophysical Research – Atmospheres*, Vol. 105, No. D9, pp. 11879–11888.

Ni, W., Li, X.W., Woodcock, C.E., Roujean, J.L., and Davis, R.E. 1997. Transmission of solar radiation in boreal conifer forests: measurements and models. *Journal of Geophysical Research – Atmospheres*, Vol. 102, No. D24, pp. 29555–29566.

Ni, W., Li, X.W., Woodcock, C.E., Caetano, M.R., and Strahler, A.H. 1999a. An analytical hybrid GORT model for bidirectional reflectance over discontinuous plant canopies. *IEEE Transactions on Geoscience and Remote Sensing*, Vol. 37, No. 2, pp. 987–999.

Ni, W., Woodcock, C.E., and Jupp, D.L.B. 1999b. Variance in bidirectional reflectance over discontinuous plant canopies. *Remote Sensing of Environment*, Vol. 69, No. 1, pp. 1–15.

Ni-Meister, W., Jupp, D.L.B., and Dubayah, R. 2001. Modeling lidar waveforms in heterogeneous and discrete canopies. *IEEE Transactions on Geoscience and Remote Sensing*, Vol. 39, No. 9, pp. 1943–1958.

Nilson, T. 1999. Inversion of gap frequency data in forest stands. *Agricultural and Forest Meteorology*, Vol. 98–99, pp. 437–448.

Patenaude, G., Hill, R.A., Milne, R., Gaveau, D.L.A., Briggs, B.B.J., and Dawson, T.P. 2004. Quantifying forest above ground carbon content using LiDAR remote sensing. *Remote Sensing of Environment*, Vol. 93, No. 3, pp. 368–380.

Serra, J. 1982. *Image analysis and mathematical morphology.* Academic Press, London.

Song, C.H., and Woodcock, C.E. 2002. The spatial manifestation of forest succession in optical imagery – the potential of multiresolution imagery. Remote Sensing of Environment, Vol. 82, Nos. 2–3, pp. 271–284.

Song, C.H., and Woodcock, C.E. 2003. Monitoring forest succession with multitemporal Landsat images: factors of uncertainty. *IEEE Transactions on Geoscience and Remote Sensing*, Vol. 41, No. 11, pp. 2557–2567.

Song, C.H., Woodcock, C.E., and Li, X.W. 2002. The spectral/temporal manifestation of forest succession in optical imagery – the potential of multitemporal imagery. *Remote Sensing of Environment*, Vol. 82, Nos. 2–3, pp. 285–302.

Strahler, A.H., and Jupp, D.L.B. 1990. Geometric-optical modeling of forests as scenes composed of three-dimensional discrete objects. In *Photon-vegetation interactions: applications in optical remote sensing and plant ecology.* Edited by R.B. Myneni and J. Ross. Springer-Verlag, Heidelberg, FRG. pp. 415–440.

Strahler, A.H., Jupp, D.L.B., Woodcock, C.E., Schaaf, C.B., Yao, T., Zhao, F., et al. 2008. Retrieval of forest structural parameters using a ground-based lidar instrument (Echidna®). *Canadian Journal of Remote Sensing*, Vol. 34, Suppl. 2. This issue.

Zwally, H.J., Schutz, B., Abdalati, W., Abshire, J., Bentley, C., Brenner, A., et al. 2002. ICESat's laser measurements of polar ice, atmosphere, ocean, and land. *Journal of Geodynamics*, Vol. 34, Nos. 3–4, pp. 405–445.